Metrol. Meas. Syst., Vol. 29 (2022) No. 1, pp. 207–229
DOI: 10.24425/mms.2022.138542

PAN POLSKA AKADEMIA NAUK

METROLOGY AND MEASUREMENT SYSTEMS

Index 330930, ISSN 0860-8229
www.metrology.wat.edu.pl

M&MS

A COMPREHENSIVE CYCLOID PIN-WHEEL PRECISION REDUCER TEST PLATFORM INTEGRATED WITH A NEW DYNAMIC MEASUREMENT METHOD OF LOST MOTION

Huijun Yue, Xiangkai Wu, Zhaoyao Shi, Yue Zhang, Yong Ye, Lintao Zhang, Ying Fu

Beijing University of Technology, Beijing Engineering Research Center of Precision Measurement Technology and Instruments, 100, Ping Le Yuan, Chaoyang District, Beijing 100124, China, (*yuehj@bjut.edu.cn, wxk@emails.bjut.edu.cn,* ✉ *shizhaoyao@bjut.edu.cn,* +86 010 6739 2894, *zhangy0921@163.com. 13540286169@126.com, 18982072228@163.com, 13608042599@126.com*)

Abstract

While cycloid pin-wheel precision reducers (referred to as RV reducers) are widely used in industrial robots, a widely accepted design standard or verification method of their test platforms is not available. In this study, a comprehensive sliding-separation test platform of RV reducers was developed. The test platform can test various measurement items such as transmission error, static measurement of lost motion, dynamic measurement of lost motion, torsional rigidity, no-load running torque, starting torque, backdriving torque, and transmission efficiency of the RV reducer for robots. The principle and method of dynamic measurement of lost motion tests based on the two-way transmission error method were studied and this test function was successfully integrated with the comprehensive test platform in order to increase the test items of the dynamic performance parameters of RV reducers. The measurement results of the no-load running torque of the RV reducer were consistent with the Stribeck curve. Based on the concept of optimal measurement speed, a decomposition test method of the geometric component of the dynamic measurement of lost motion and the elastic component of the dynamic measurement of lost motion was proposed in the dynamic measurement test of lost motion. Through precision calibration, function test and repeatability test, the results were compared with the data of enterprise's samples. The consistent results have proved that the test platform met engineering requirements and measurement accuracy requirements. Based on the new test principle, the developed platform can test more parameters of RV reducers with high precision and display the comprehensive test performance.

Keywords: cycloid pin-wheel precision reducer (RV reducer), test platform, comprehensive performance, dynamic measurement of lost motion, decomposition test method.

1. Introduction

Due to continuous improvements on the industrial level in recent years, the demand for advanced intelligent equipment, especially industrial robots, has increased year by year [1]. As the RV reducer is the core component of an industrial robot and its performance directly affects

Article history: received June 22, 2021; revised August 4, 2021; accepted August 24, 2021; available online October 17, 2021.

the overall performance of a robot [2], it is necessary to carry out the comprehensive tests of performance parameters of RV reducers in order to improve their design and processing level.

Many scholars have explored the performance and testing of precision reducers. Blagojevic, Kudrijavcev and Bednarczyk explored the internal structure, the force and deformation of components of cycloidal gear reducers [3–5]. Bogucki *et al.* proposed a new method of measuring the planet load of planetary gear sets, in which strain gauges mounted directly on the planet pins were used to continuously measure the loads carried by the planets assembled in a fixed carrier [6]. Yang *et al.* developed a test bed to conduct a large number of experiments on the transmission efficiency and temperature rise of a cycloid pin-wheel reducer [7]. Li and Wang developed a comprehensive test system to explore the key performance indicators in a variety of precision reducers [8]. The test system designed by Zheng *et al.* was used to measure the speed, torque and other parameters of cycloid pin-wheel reducers [9]. Gorla *et al.* measured the transmission efficiency of cycloid pin-wheel reducers [10]. Jorgensen *et al.* designed a cycloid reducer utilizing permanent magnet gears and tested its transmission efficiency [11]. Nam and Oh designed an RV reducer with a trapezoidal profile and established a test platform to test the transmission accuracy and torsional rigidity of the reducer [12]. Fan *et al.* developed a static test system to measure the hysteresis curve, torsional rigidity, lost motion, torsion curve, ultimate torque and other parameters of the precision planetary servo reducer [13]. Li *et al.* developed a lost motion and stiffness test device for 2K-V reducers [14]. Zhang *et al*. designed an automated test platform for harmonic reducers which achieved the high-precision measurements of the preload, starting torque, no-load running torque and shaft stiffness of the harmonic reducer [15]. Qi *et al.* designed a comprehensive performance test platform for RV reducers which can quickly and accurately obtain the transmission error, no-load running torque, and lost motion of RV reducers [16]. Cao *et al.* proposed a new RV test platform with a horizontal axial structure, analyzed the strain of the test platform under loading conditions and studied the effect of coaxiality on transmission errors [17].

Existing test platforms meet the requirements of testing some performance parameters of RV reducers to a certain degree but most of them have a single test function, instable measurement loads and low measurement accuracy. In addition, the mechanical structure of the test bench for testing multiple parameters is complex. Therefore, it is necessary to develop a comprehensive performance test platform for RV reducers for robots by combining new principles and methods with traditional test items in order to realize high-precision and comprehensive tests of dynamic performance parameters in RV reducers under the conditions of different speeds and different loads [18–20].

The dynamic performance of an RV reducer is particularly important in its evaluation [21, 22]. This paper explored the principles and methods of the dynamic measurement and the decomposition measurement of the lost motion and integrated these measurement functions into a comprehensive test platform.

Firstly, the concept of optimal measurement speed was proposed and both the geometric and elastic component of the dynamic measurement of lost motion were studied. Secondly, based on test principles and methods of comprehensive performance parameters of RV reducers including transmission error, lost motion (dynamic measurement and static measurement), torsional rigidity, no-load running torque, starting torque, backdriving torque and transmission efficiency, according to the requirements in the National Standard *GB/T35089-2018 Precision Gear Transmission for Robots: Test Method*, we analyzed and designed the overall scheme of the sliding-separated platform. Thirdly, the three parts including the precision mechanical system, the measurement and control system and the upper computer software system of the test platform were designed in detail. Finally, the precision calibration and repeatability tests of the

Metrol. Meas. Syst., Vol. 29 (2022), No. 1, pp. 207–229
DOI: 10.24425/mms.2022.138542

comprehensive RV reducer test platform were carried out and the function test and comparative analysis were completed. The test platform can accurately measure multiple items through simple operations. In addition, based on the concept of optimal measurement speed proposed by our team, the effects of elastic deformation and geometric dimensions were decomposed to enrich the dynamic measurement items of precision reducers. Based on the decomposition results, dynamic measurement results affected respectively by the factors of design, processing and assembly could be obtained. The test platform is of great significance to the performance improvement of precision reducers.

2. Dynamic measurement and decomposition principle of lost motion

2.1. Dynamic measurement principle and method of lost motion

The two-way transmission error method was used for dynamic measurement of lost motion of an RV reducer. Under no-load or constant load conditions, the forward and reverse transmission error curves were measured and the grating zero signal was used to ensure the consistent measurement position of the forward and reverse transmission error curves. The difference between the reverse transmission error curve and the forward transmission error curve was obtained to plot the dynamic measurement curve of lost motion (Fig. 1).

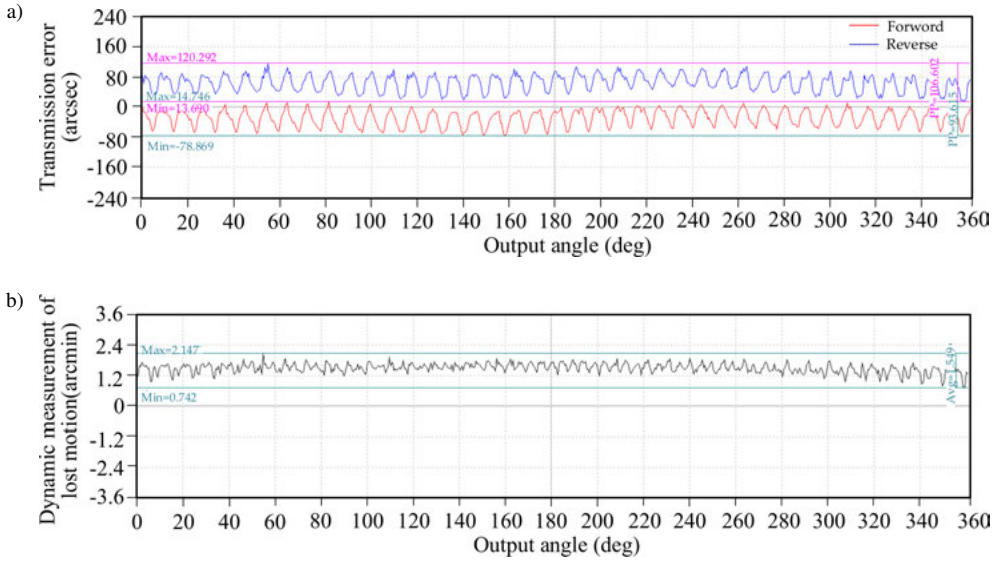

Fig. 1. Process of obtaining the dynamic measurement curve of the lost motion: a) Forward and reverse transmission errors; b) Dynamic measurement curve of the lost motion.

The operating principle of dynamic measurement of lost motion is introduced below. After the RV reducer is installed, the comprehensive test platform (see Section 3) drives the RV reducer forward and the output terminal of the reducer rotates 360°. The position of the circle grating at 360° is marked at the same time. Based on the measurement data of the input and output circular gratings, with the speed ratio of the RV reducer, the forward transmission error of one rotation of the output terminal is calculated. After the test platform continues to drive the RV reducer

forward to a certain angle, the RV reducer rotates in the direction reverse to the marked position of the circle grating at 360° to ensure that the end point of the forward rotation and the starting point of the reverse rotation are the same. The test platform continues to drive the RV reducer in the reverse direction. After the output terminal of the reducer rotates 360°, the measurement data of the input and output circular gratings are combined with the speed ratio of the RV reducer to calculate the reverse transmission error of one rotation of the output terminal. The abscissas of the curve of the forward transmission error and the reverse transmission error obtained in this way are aligned and the two curves can be directly subtracted.

In Fig. 1a, the blue line is the transmission error curve of the reducer's reverse rotation and the red line is the transmission error curve of the reducer's forward rotation. It can be seen that the periodicity of the two curves is the same and that the fluctuation range is similar. The difference between the two curves is the dynamic measurement result of the lost motion, as shown in Fig. 1b.

2.2. Decomposition of the dynamic measurement result of lost motion

The influencing factors of dynamic measurement of lost motions of RV reducer can be classified either as internal factors (design, processing, assembly, *etc.*) or external factors (speed, torque, temperature, *etc.*). Our research team decomposed the generalized results of dynamic measurement of lost motion of RV reducers into a geometric component and an elastic component.

The no-load friction characteristic curve of an RV reducer shows a typical Stribeck effect [23]. Under no-load conditions, the lost motion (dynamic measurement) measured at the speed corresponding to the minimum friction point in the friction characteristic curve is defined as the geometric component. This speed is defined as the optimal speed for transmission error measurement and dynamic measurement of lost motion. The elastic component is defined as the difference between the generalized result of dynamic measurement of lost motion and the geometric component under load conditions [24]:

$$\delta = \delta g + \delta e, \tag{1}$$

where δ, δg and δe, respectively, are the result of dynamic measurement of lost motion, the geometric component and the elastic component.

Fig. 2a shows the result of dynamic measurement of lost motion under load conditions and Fig. 2b shows the geometric component at optimal measurement speed. The zero signal of the grating is used to ensure the consistency of the measurement position. The difference of two curves (Fig. 2a and Fig. 2b) is the elastic component in the result of the dynamic measurement of lost motion.

a)

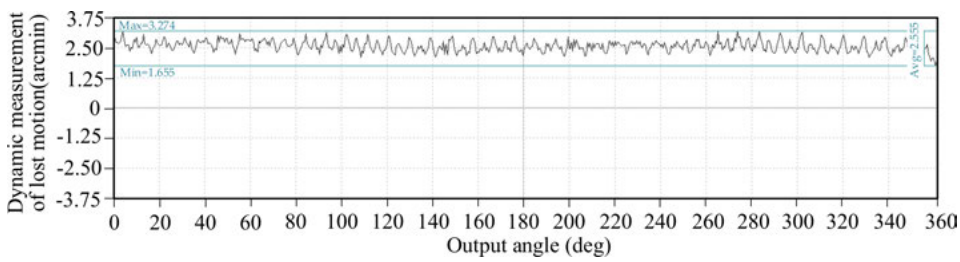

Fig. 2a

Metrol. Meas. Syst., Vol. 29 (2022), No. 1, pp. 207–229
DOI: 10.24425/mms.2022.138542

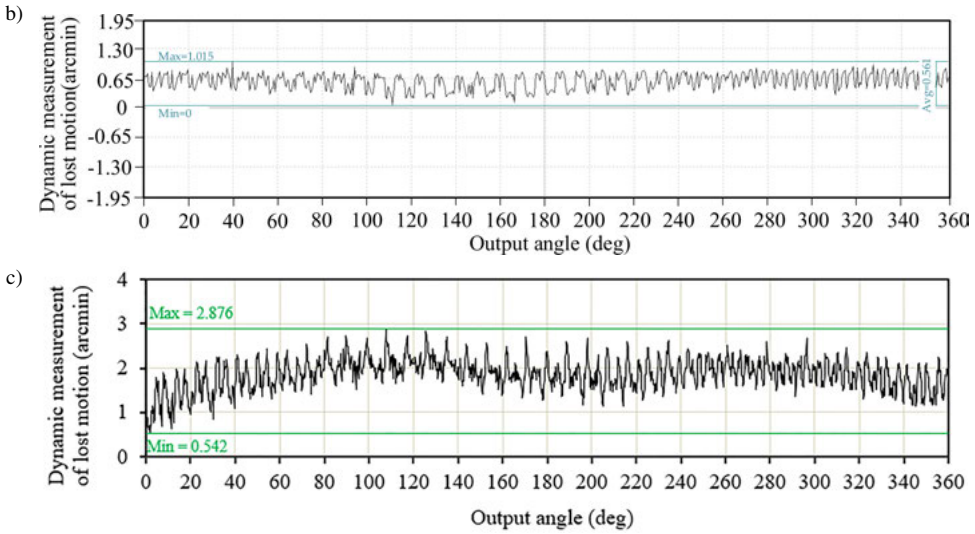

Fig. 2. Dynamic measurement curve of lost motion: a) Results of dynamic measurement of lost motion; b) Geometric component of dynamic measurement of lost motion; c) Elastic component of dynamic measurement of lost motion.

3. Overall scheme of the test platform

3.1. Overall requirements

RV reducers have many specifications, covering a wide range of speed and torque. In order to meet the requirements of high accuracy and simple operation, the technical indicators of RV reducers to be tested in this test platform are provided as follows:

1. RV reducer with a maximum output torque of 1500 N·m;
2. Speed ratio: $\leq$ 121;
3. Range of input shaft speed: 0-3000 r/min;
4. Torque sensor measuring accuracy: ±0.1% F.S;
5. Grating measuring accuracy: ±1″;
6. Test items: transmission error (no-load and constant load), lost motion (dynamic measurement and static measurement), torsional rigidity, *etc*. The details are shown in Table 1.

Table 1. Test items.

Test items	Test contents	Units of measurements
Transmission error	No-load transmission error	arcsec
	Load transmission error	arcsec
Lost motion	Dynamic measurement of lost motion	arcsec
	Elastic component (dynamic measurement) Geometric component (dynamic measurement)	arcsec
	Static measurement of lost motion	arcsec
Torsional rigidly	Torsional rigidly	N·m/acrmin
Torque	No-load running torque	cN·m
	Starting torque	N·m
	Backdriving torque	cN·m
Transmission efficiency	Transmission efficiency	%

3.2. Overall design

The comprehensive RV reducer test platform adopted a sliding-separation design so that the test of multiple items could be completed through the separation and combination of various precision platforms. The test platform is mainly composed of three parts: precision mechanical system, measurement and control system and an upper computer software system. The main body of the test platform adopted a horizontal structure scheme, as shown in Fig. 3.

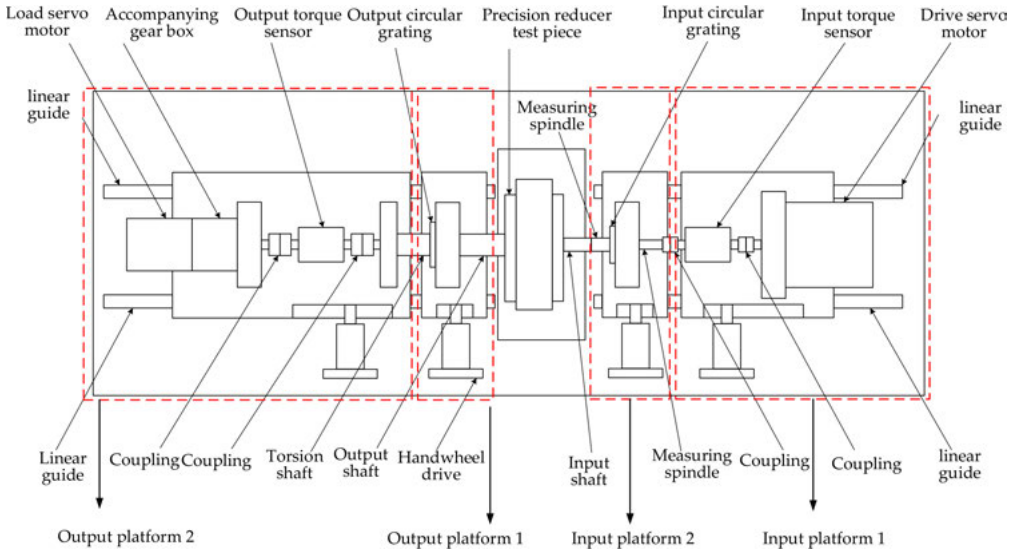

Fig. 3. Schematic diagram of the main body of the platform.

The input terminal is on the right and the output terminal is on the left side. The main components of the test platform from right to left are respectively the drive servo motor, input torque sensor, circular input grating, precision reducer test piece, circular output grating, output torque sensor, accompanying gearbox, and load servo motor. The tested RV reducer is fixed with the bracket and other precision platforms can be moved along the linear guide to realize the measurements of different measurement items.

3.3. Sub-item measurement

Through the separation and combination of 4 precision platforms, the multi-item measurement can be realized, as shown in Fig. 4.

As shown in Fig. 4, when the no-load transmission error, no-load dynamic measurement of lost motion, starting torque, or no-load running torque is measured, the No. 2 output platform does not participate in the test process. All the platforms are engaged in the test process of load transmission error, loading dynamic measurement of lost motion, or transmission efficiency. When the backdriving torque is measured, the No. 1 input platform does not participate in the test process. When torsional rigidity or static measurement of lost motion is measured, the No. 1 or No. 2 input platform do not participate in the test process and the input terminal of the RV reducer is fixed.

Metrol. Meas. Syst., Vol. 29 (2022), No. 1, pp. 207–229
DOI: 10.24425/mms.2022.138542

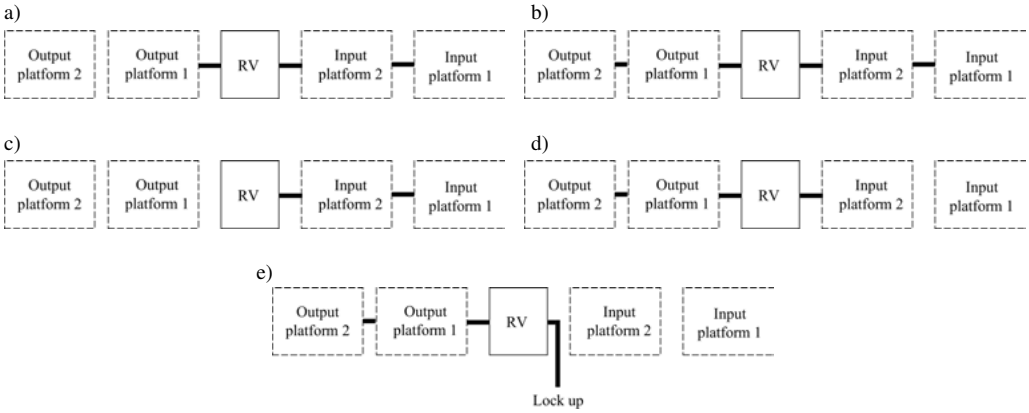

Fig. 4. Measurement items: a) No-load transmission error, no-load dynamic measurement of lost motion, and starting torque; b) Load transmission error, load dynamic measurement of lost motion, and transmission efficiency; c) No-load running torque; d) Backdriving torque; e) Torsional rigidity and static measurement of lost motion.

3.4. Working principle

The working principle of the test platform is shown in Fig. 5 [25].

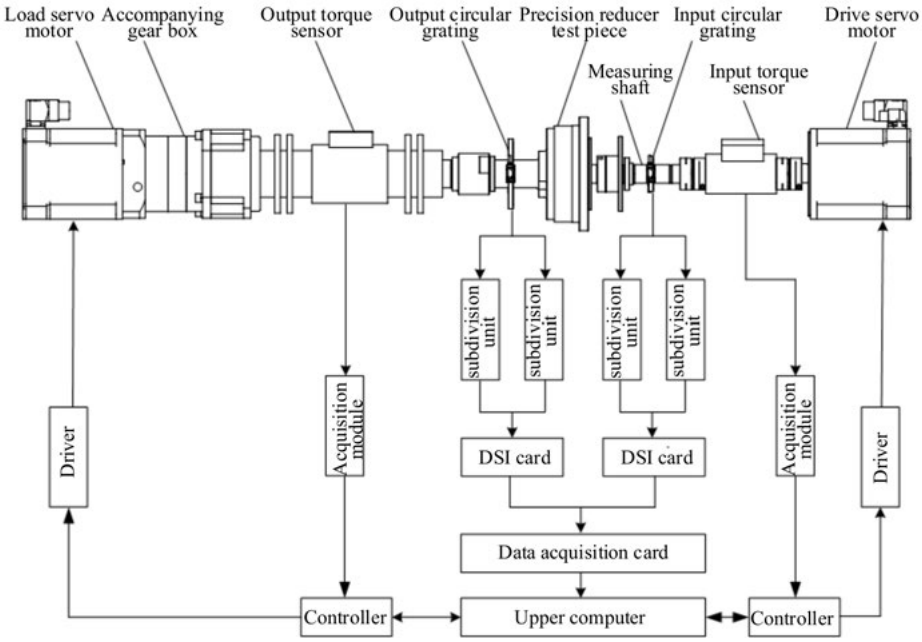

Fig. 5. Working principle of the test platform.

The circular grating uploads the angular displacement information to the upper computer through the reading head, subdivision unit, DSI card and data acquisition card. The torque sensor uploads the data to the upper computer via the acquisition module. The upper computer controls

the drive servo motor and the load servo motor to respectively drive and apply loads onto the shaft system of the test platform. The upper computer software analyzes the collected data and outputs the measurement curve and test results.

4. Sub-system design

4.1. Precision mechanical system

The precision mechanical system is shown in Fig. 6. The test platform is divided into five parts, as shown in Table 2. Each component is installed on a cast iron base with a precision bracket

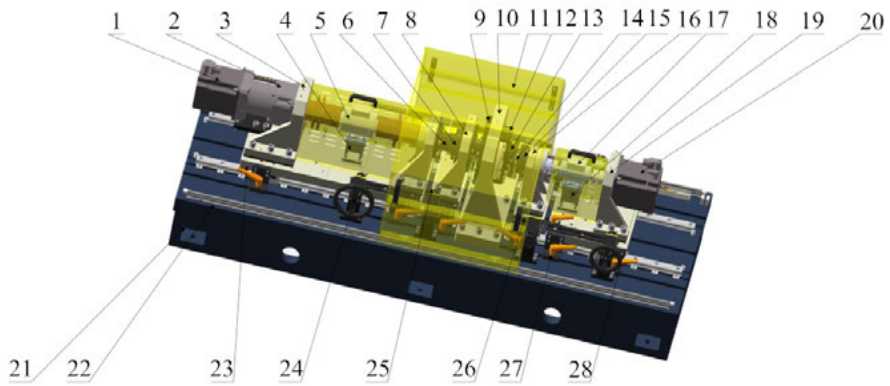

Fig. 6. Precision mechanical system. 1. Load servo motor, 2. Accompanying gear box, 3. No. 6 precision bracket, 4. No. 5 precision bracket, 5. Output torque sensor, 6. Torsion shaft, 7. Output circular grating, 8. No. 4 precision bracket, 9. Precision reducer test piece, 10. RV reducer mounting bracket, 11. Shield, 12. Input shaft fixing mechanism, 13. RV reducer input shaft, 14. Measuring shaft, 15. Input circular grating, 16. No. 3 precision bracket, 17. Input torque sensor, 18. No. 2 precision bracket, 19. No. 1 precision bracket, 20. Drive servo motor, 21. Cast iron base, 22. Linear guide, 23. No. 4 precision skateboard, 24. Handwheel drive, 25. No. 3 precision skateboard, 26. No. 2 precision skateboard, 27. Locker.

Table 2. Components of the test platform.

Platform No.	Platform names	Components
1	RV reducer installation components	RV reducer mounting bracket, precision reducer test piece (including the output shaft), and input shaft fixing mechanism.
2	Input platform 1	Drive servo motor, input torque sensor (±0.02 N·m), No. 1 precision bracket (motor), No. 2 precision bracket (torque sensor), and No. 1 precision skateboard.
3	Input platform 2	Measuring shaft, input circular grating (±1 arcsec), RV reducer input shaft, No. 3 precision bracket (grating), and No. 2 precision skateboard.
4	Output platform 1	Output circular grating (±1 arcsec), No. 4 precision bracket (grating), and No. 3 precision skateboard.
5	Output platform 2	Torsion shaft, Output torque sensor (±2 N·m), accompanying gear box, load servo motor, No. 5 precision bracket (torque sensor), No. 6 precision bracket (accompanying test gear box), and No. 4 precision skateboard.

Metrol. Meas. Syst., Vol. 29 (2022), No. 1, pp. 207–229
DOI: 10.24425/mms.2022.138542

and a precision skateboard. Each precision mobile platform is equipped with a locker to ensure the stability of the test platform. Outer shields are also designed for the test rotating mechanism in order to ensure the safety of the test platform.

4.2. Measurement and control system

The measurement and control system is mainly composed of a motion control module and a data acquisition module. The principal block diagram is shown in Fig. 7.

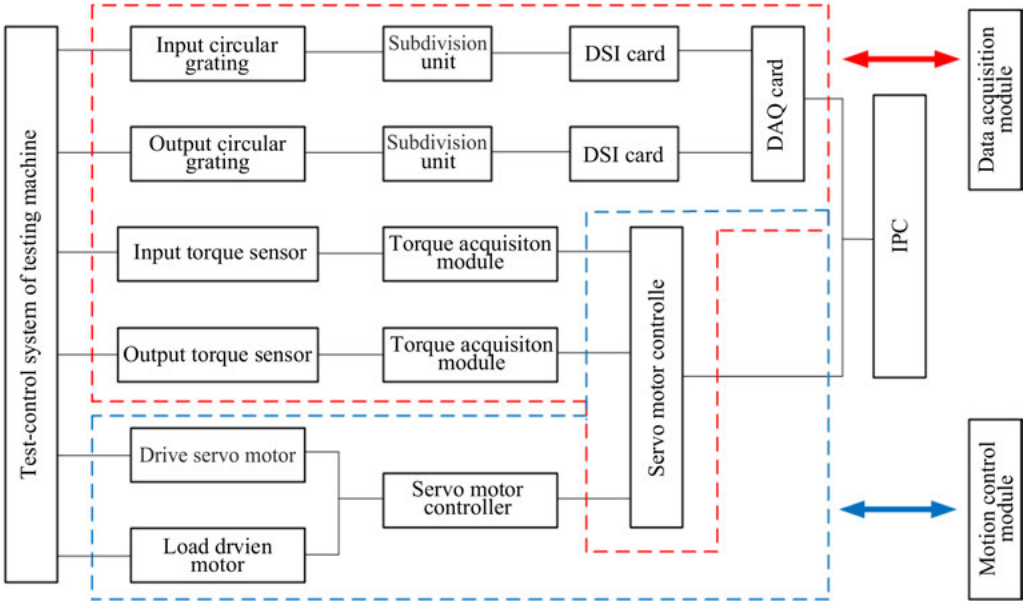

Fig. 7. Block diagram of the measurement and control system.

In the test platform, the rotation movement of the RV reducer shaft system and the application of the load at the output terminal are realized via the motion control module. The parameters such as rotation direction, speed and load are set in the measurement software according to the measurement requirements so that the operation of the servo motor can be precisely controlled. The measured data are uploaded to the upper computer software via the data acquisition module.

4.3. Measurement and control software

The overall framework of the test platform software is shown in Fig. 8 [25]. The measurement software of the comprehensive RV reducer test platform includes 5 modules: the parameter management module, control test module, measurement module, data management module and report printing module.

The software parameter setting and test interface are shown in Fig. 9.

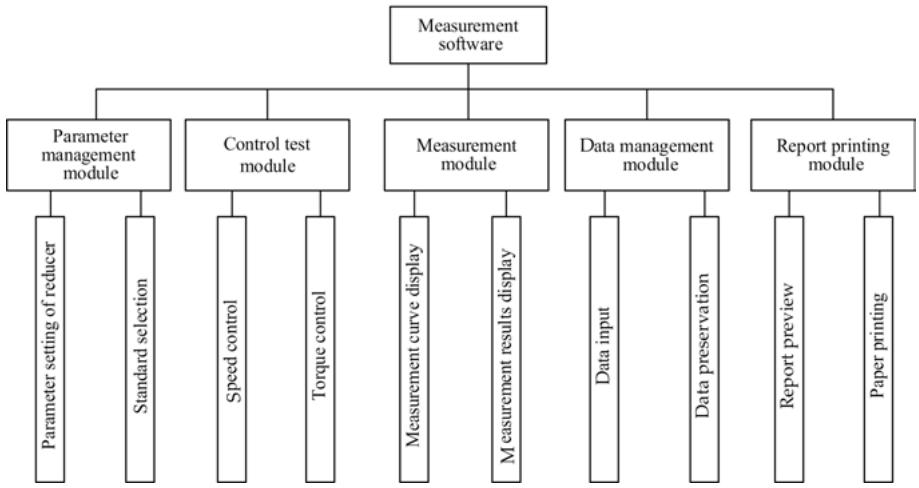

Fig. 8. Framework diagram of the measurement and control software.

a)

b)

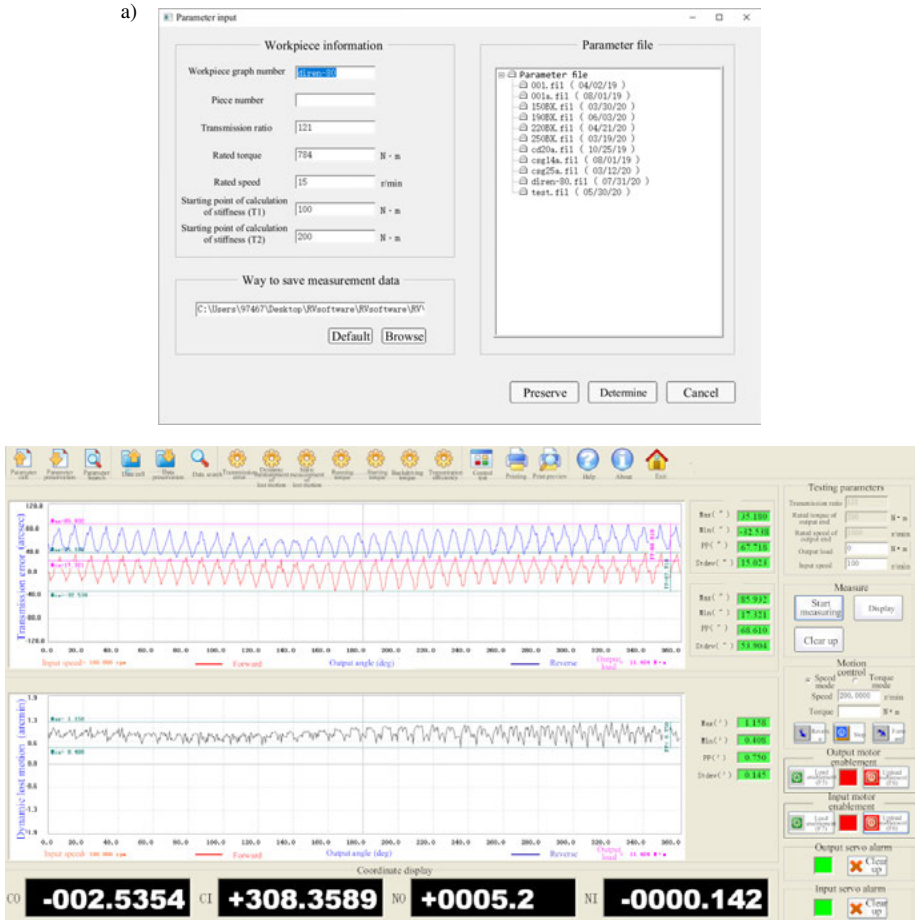

Fig. 9. Software interface: a) Parameter setting; b) Measurement interface.

Metrol. Meas. Syst., Vol. 29 (2022), No. 1, pp. 207–229
DOI: 10.24425/mms.2022.138542

5. Precision calibration and measurement uncertainty analysis

The test platform has been commercialized and applied in many research institutions. Its photos are shown in Figs. 10 and 11. The test platform shown in Figure 11 was adopted in the measurement and analysis below.

a) b)

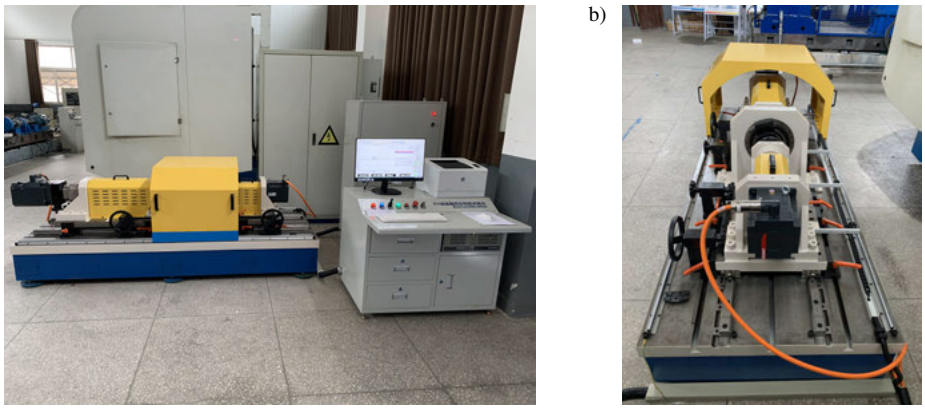

Fig. 10. No. 1 test platform prototype: a) overall view and b) precision machinery part.

a) b)

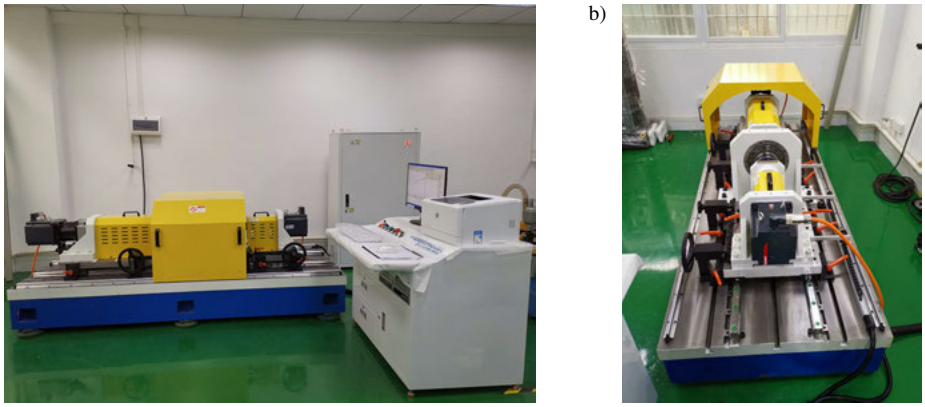

Fig. 11. No. 2 test platform prototype: a) overall view and b) precision machinery part.

5.1. System precision calibration

The installation accuracy of the mechanical system of the test platform was calibrated to ensure that the measurement stability of the test platform met the requirements. The results are shown in Table 3.

The RV reducer was replaced with a shaft that met the rigidity requirements. Under the transmission ratio of 1, the measurement precision was calibrated (Table 4).

The maximum relative error was 4.6% and the maximum standard deviation was 0.1769 arcsec, indicating that the measurement result was accurate.

Table 3. Calibration results of the mechanical system.

Calibration items	Measured values	Design requirements	Calibration results
Shafting contour calibration	2 μm/100 mm	Value change ≤ 6 μm/100 mm	Qualified
Shafting coaxiality verification	The coaxiality of input shaft and output shaft is 6 μm	Value change ≤ 6 μm/100 mm	Qualified
Radial runout of shafting	The radial runout of the input shaft is 2 μm/100 mm and the radial runout of the output shaft is 4 μm/100 mm;	Value change ≤ 5 μm/100 mm	Qualified
End face runout of shafting	The end face runouts of the input shaft and the output shaft are respectively 4 μm/100 mm and 5 μm/100 mm.	Value change ≤ 5 μm/100 mm	Qualified

Table 4. Calibration results of the shaft transmission error.

Serial numbers	Fluctuation amplitude of reverse transmission error (arcsec)	Relative error (%)	Fluctuation amplitude of forward transmission error (arcsec)	Relative error (%)
1	6.387	2.7%	7.552	0.40%
2	6.139	1.2%	7.653	0.93%
3	6.310	1.5%	7.457	1.66%
4	6.155	0.97%	7.822	3.16%
5	6.231	0.26%	7.928	4.6%
6	5.958	4.3%	7.510	0.96%
7	6.439	3.5%	7.569	0.18%
8	6.108	1.7%	7.473	1.4%
9	6.139	1.2%	7.531	0.68%
10	6.280	1.0%	7.331	3.3%
Average values	6.215	–	7.583	–
Standard deviation	0.1437	–	0.1769	–

5.2. System repeatability

A certain type of RV reducer (whose transmission ratio is 121) of a certain manufacturer was tested in the study. The multiple measurement results of dynamic measurement of lost motion under the no-load condition and at a speed of 100 r/min are shown in Table 5.

The standard deviation of multiple measurements of lost motion (dynamic measurement) fluctuation amplitude was 0.0419 arcmin. The standard deviation of multiple measurements of average values of lost motion (dynamic measurement) was 0.0221 arcmin, indicating that the results had good repeatability.

Metrol. Meas. Syst., Vol. 29 (2022), No. 1, pp. 207–229
DOI: 10.24425/mms.2022.138542

Table 5. Dynamic measurement of lost motion repeatability.

Serial numbers	**Fluctuation amplitude of dynamic measurement of lost motion (arcmin)**	**Average values of dynamic measurement of lost motion (arcmin)**
1	0.923	0.530
2	0.994	0.573
3	0.903	0.509
4	0.950	0.554
5	0.957	0.502
6	1.005	0.519
7	1.015	0.522
8	0.927	0.525
9	1.021	0.561
10	1.015	0.545
Average values	0.971	0.534
Standard deviation	0.0419	0.0221

6. Test and data analysis

A certain type of RV reducer (whose transmission ratio is 121) was tested in the study.

6.1. No-load running torque

Under the conditions of a load of 0 N·m, the no-load running torque curve was plotted (Fig. 12).

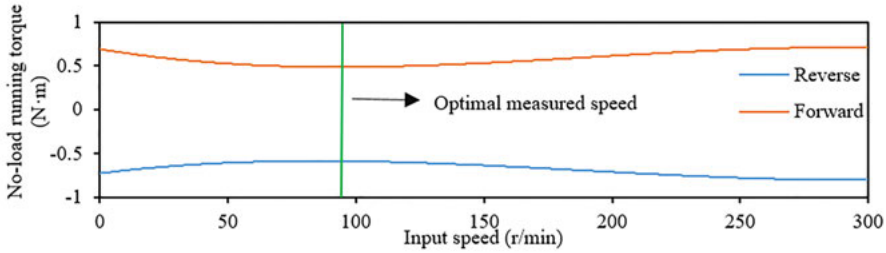

Fig. 12. No-load running torque.

The curve of the no-load running torque of the RV reducer is a parabola. With the increase in the speed, the no-load running torque firstly decreases and then gradually increases. Therefore, the friction characteristic of the RV reducer has a typical Stribeck effect. When the speed was about 100 r/min, the no-load running torque was the smallest (0.48 N·m under the forward rotation conditions and –0.56 N·m under the reverse rotation conditions). The optimal measurement speed for this RV reducer was determined as 100 r/min.

Therefore, the operating conditions of the RV reducer combined with the measured friction characteristics can effectively guide the design of the RV reducer.

6.2. Transmission error test

In order to analyze the influences of geometric factors on the transmission error of the RV reducer, the optimal measurement speed was adopted in the measurement of the no-load transmission error. Under the no-load condition and at a speed of 100 r/min, the transmission error curve was plotted (Fig. 13).

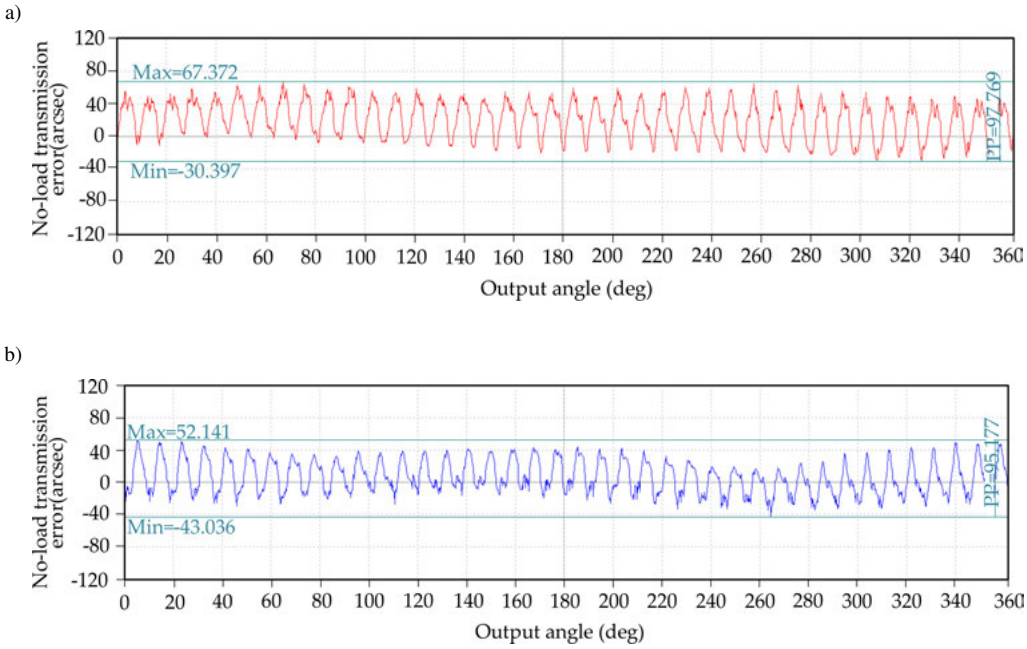

Fig. 13. No-load transmission error curves: a) forward no-load transmission error and b) reverse no-load transmission.

The comprehensive test platform can also measure the transmission error of the RV reducer under load conditions. (Fig. 14) was plotted at a speed of 100 r/min and under a load of 100 N·m, the transmission error curve.

The peak values of the forward no-load transmission error were 67.372″ and −30.397″ and the fluctuation range was 97.769″ (Fig. 13a). The peak values of the reverse no-load transmission error were 52.141″ and −43.036″ and the fluctuation range was 95.177″ (Fig. 13b).

It can be seen that the periodic pattern of forward and reverse transmission errors was the same and that the fluctuation range difference was 1.34%.

The peak values of forward transmission error under a load of 100 N·m were 43.324″ and −52.851″ and the fluctuation range was 96.175″ (Fig. 14a). The peak values of reverse transmission error under the load of 100 N·m were 53.153″ and −62.872″ and the fluctuation range was 116.025″ (Fig. 14b). Based on the measurement data, this RV reducer could be analyzed and evaluated from the aspects of machining accuracy and load deformation.

Metrol. Meas. Syst., Vol. 29 (2022), No. 1, pp. 207–229
DOI: 10.24425/mms.2022.138542

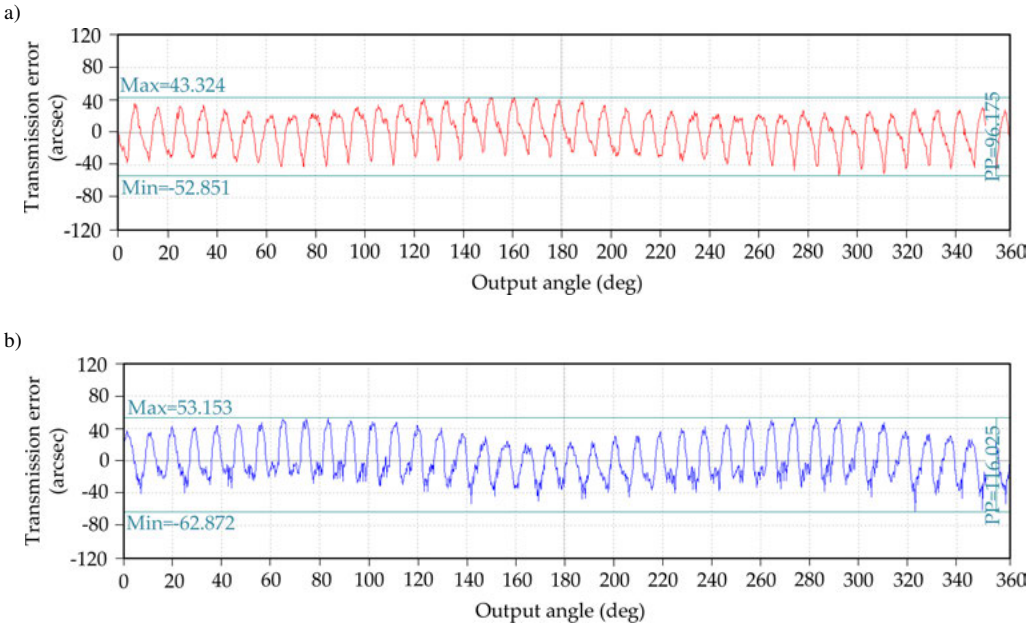

Fig. 14. Transmission error curves under a load of 100 N·m: a) forward load transmission error and b) reverse load transmission error.

6.3. Dynamic measurement test of lost motion

The dynamic measurement test of lost motion was performed according to the two-way transmission error method. Firstly, the transmission error of the RV reducer was measured in the forward direction (output 0°–360°). Then, the output terminal continued to rotate forward to a certain angle and then rotated in the reverse direction to 360°. Finally, the transmission error of the reverse rotation was measured (output 360°–0°). During the measurement process, the forward and reverse transmission error measurement curves were aligned and a backlash factor was introduced in the measurement results. Therefore, it was different from the transmission error measurement result alone.

The difference between the reverse transmission error and the forward transmission error was the lost motion (dynamic measurement). Fig. 15 shows the geometric component of dynamic measurement of lost motion at the optimal measurement speed of 100 r/min. Fig. 16 shows the dynamic measurement of lost motion under a load of 100 N·m and at a speed of 100 r/min. Fig. 17 shows the elastic component of dynamic measurement of lost motion under a load of 100 N·m and at a speed of 100 r/min. Fig. 18 shows the fluctuation amplitude of dynamic measurement of lost motion under different speeds and loads.

It can be seen from Figs. 15–17 that under the no-load optimal speed condition, the dynamic measurement peak values of the lost motion were 0.892′ and 0.044′ and that the fluctuation range was 0.848′. As the friction effect was minimal at this time, the measurement result was mainly caused by geometric factors. Under load conditions, the peak values of the dynamic measurement of lost motion were 3.826′ and 1.832′ and the amplitude of the fluctuation was 1.454′. It can be seen that the curve moved upward as a whole and the fluctuation range became larger. The measurement difference between load and no-load conditions is the elastic component of dynamic

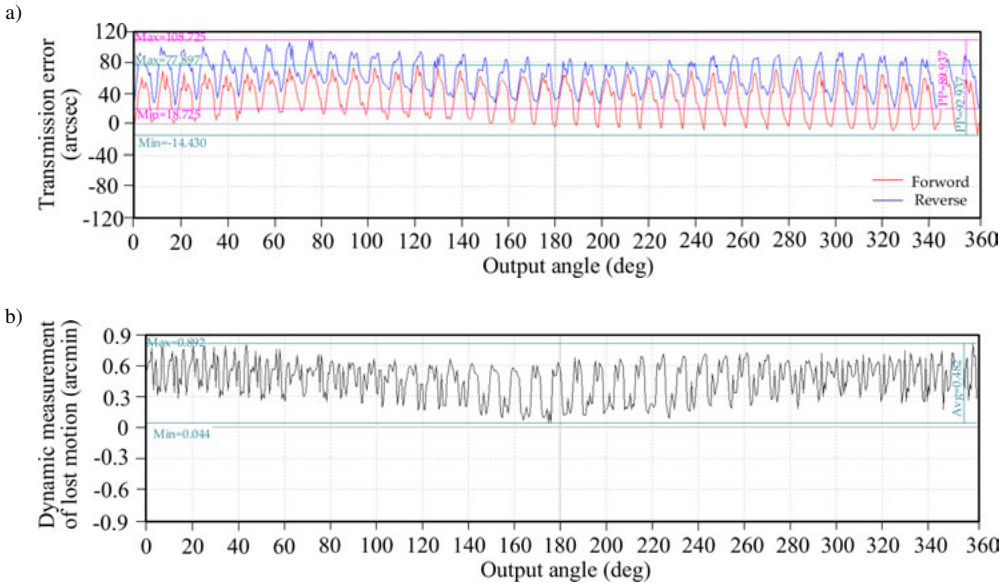

Fig. 15. Process of obtaining the dynamic measurement curve of lost motion under no-load condition: a) forward and reverse no-load transmission error and b) dynamic measurement curve of lost motion.

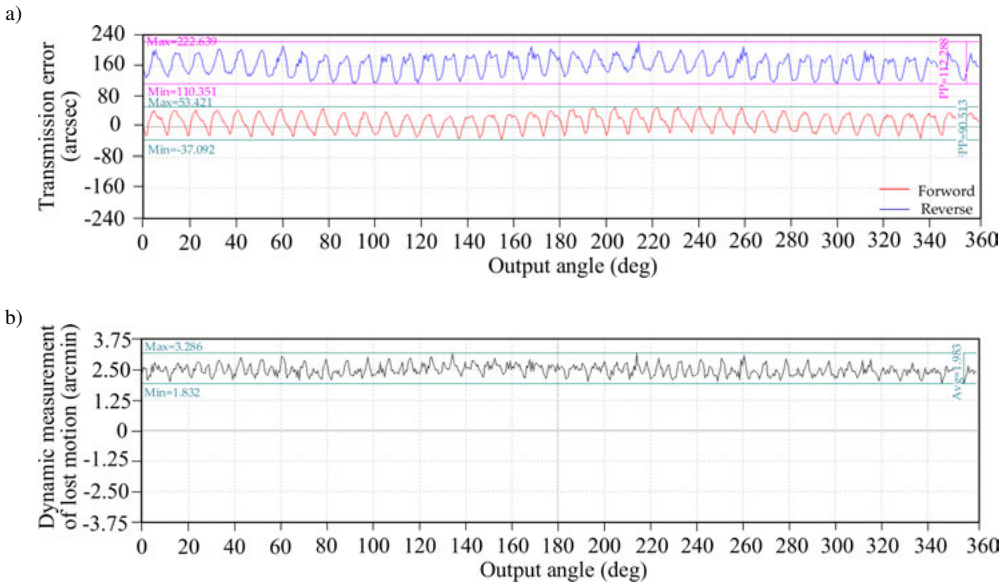

Fig. 16. Process of obtaining the dynamic measurement curve of lost motion under a load of 100 N·m: a) forward and reverse transmission errors under a load of 100 N·m and b) dynamic measurement curve of lost motion under a load of 100 N·m.

measurement of lost motion and mainly reflects the elastic deformation of the reducer under load conditions.

Metrol. Meas. Syst., Vol. 29 (2022), No. 1, pp. 207–229
DOI: 10.24425/mms.2022.138542

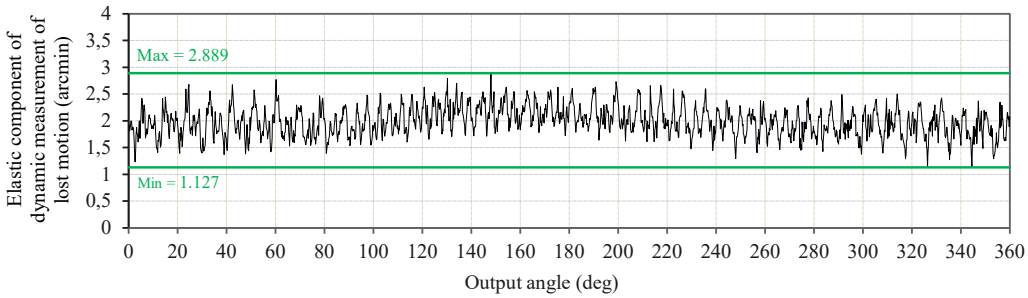

Fig. 17. Elastic component of dynamic measurement of lost motion.

At the same speed, the greater was the torque, the greater was the fluctuation amplitude of lost motion (dynamic measurement), as shown in (Fig. 18).

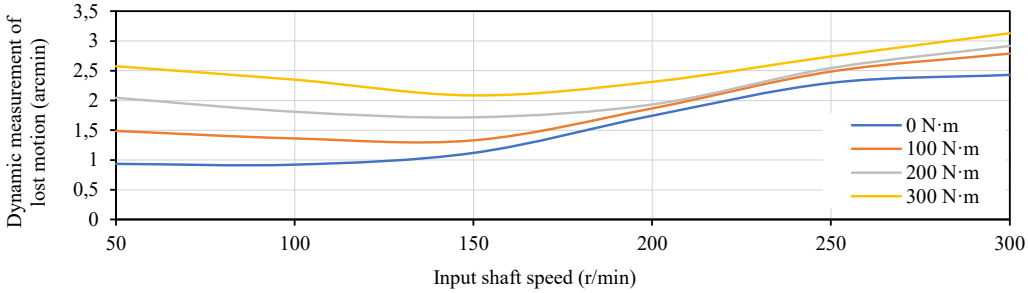

Fig. 18. Trend curves of the dynamic measurement of lost motion amplitude under different working conditions.

6.4. Static measurement test of lost motion and torsional rigidity test

When the same load was applied in the forward and reverse strokes, the torsion angles were different because the RV reducer had the hysteresis characteristics caused by its nonlinear torsional rigidity and nonlinear friction.

The hysteresis characteristics of the RV reducer were thus measured. According to the requirements of the National Standard (GB/T35089-2018 Precision Gear Transmission for Robots: Test Method), the static measurement of lost motion is defined as the absolute value of the angle difference between the midpoints of the two sets of intersections at ±3% of the rated torque on the hysteresis curve.

In the test platform, the rated torque could be applied to measure the torsional rigidity according to the National Standard (GB/T35089-2018 Precision Gear Transmission for Robots: Test Method) and the torsional rigidity value could be measured in sections (Fig. 19).

The result of static measurement of the lost motion was 0.443′. The backlash was 0.485′ and the torsional rigidity was calculated to be 141.9 N·m/arcmin directly from the hysteresis curve.

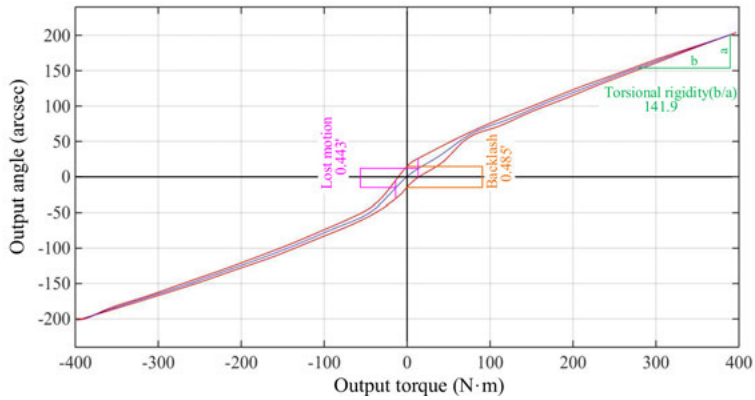

Fig. 19. Hysteresis curve.

6.5. Starting torque and backdriving torque test

When the output terminal was disconnected and the load was applied to the input terminal and slowly linearly increased, the starting torque was measured (Table 6).

Table 6. Starting torque.

Serial numbers	Forward starting torques (cN·m)	Reverse starting torques (cN·m)
1	65.62	–45.22
2	65.63	–46.18
3	68.10	–44.00
4	65.22	–45.79
5	61.67	–45.07
6	61.07	–46.22
7	65.89	–45.72
8	67.99	–48.05
9	64.75	–43.85
10	68.44	–46.07
Average values	65.44	–45.62
Standard deviation	2.381	1.142
Coefficient of variation	3.8%	2.6%

The reverse starting torque was –45.62 cN·m and the forward starting torque was 65.44 cN·m. The backdriving torque could be measured in the same way.

6.6. Transmission efficiency test

The measured transmission efficiency curves under different working conditions are shown in Fig. 20.

Metrol. Meas. Syst., Vol. 29 (2022), No. 1, pp. 207–229
DOI: 10.24425/mms.2022.138542

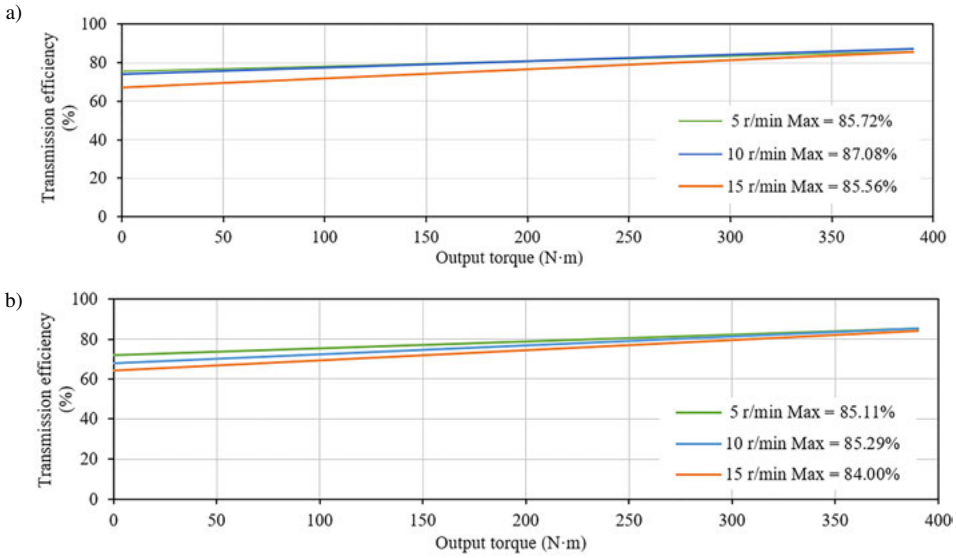

Fig. 20. Transmission efficiency curves: a) forward transmission efficiency; b) reverse transmission efficiency.

Under a rated torque of 390 N·m and at an output speed of 10 r/min, the forward transmission efficiency was the highest, 87.08%. Under a rated torque of 390 N·m and at an output speed of 10 r/min, the reverse transmission efficiency was the highest, 85.29%. At the same speed, the output efficiency increased with the increase in the output torque (Fig. 20). Under low torque conditions, the higher was the output speed, the lower was the efficiency. Under high torque conditions, the output speed change had no obvious effect on the efficiency (Fig. 20).

6.7. Comparative analysis

The measurement results were compared with the results of enterprise's sample and product manual. The comparison results are provided in Table 7.

Table 7. Comparison of measurement results.

Test items	Measurement results	Enterprise measurement results	Product manual
Static measurement of lost motion (arcmin)	0.44	0.32	≤ 1
Backlash (arcmin)	0.49	0.60	≤ 1
Efficiency (15 r/min, 390 N·m)	85.56%	85.4%	80%
Torsional stiffness (N·m/arcmin)	141.9	149	108
No-load running torque at 20° (N·m)	0.56	–	0.6

It can be seen that the measurement results of the comprehensive performance test platform were well consistent with the enterprise's samples and that the platform supported the test of dynamic measurement of lost motion. The measurement results of the experimental platform

can effectively evaluate the product performance and guide the product design and production process.

7. Conclusions

A comprehensive performance test platform for robot RV reducers, which can test transmission error, lost motion (static measurement and dynamic measurement), torsional rigidity, no-load running torque, starting torque, backdriving torque and transmission efficiency, has been developed as a result of the study. The platform has serialized extension capabilities and has been applied at a number of universities and research institutions. The main research content and significance are as follows:

Firstly, the selection principle of the optimal measurement speed for transmission error and dynamic measurement of lost motion was analyzed and the principle and test method of decomposition components of dynamic measurement of lost motion were studied. The influences of geometric quantity and elastic deformation on measurement results were respectively considered in the test method. The geometric component of dynamic measurement of lost motion is mainly used to analyze the design accuracy and processing accuracy of RV reducers, whereas the elastic component of dynamic measurement of lost motion is mainly used to analyze the influence of the load on the performance of the RV reducer.

Secondly, the test platform was composed of a precision mechanical system, a measurement and control system as well as measurement and control software. The test platform met the requirements in GB/T35089-2018 Precision Gear Transmission for Robots: Test Method and included the new functions of dynamic measurement of lost motion, geometric component of dynamic measurement of lost motion and elastic component of dynamic measurement of lost motion. The dynamic performance analysis results for RV reducers were improved. It put forward a new concept of dynamic measurement parameters, deeply explored the measurement principle and measurement method, and successfully integrated this measurement function into a test platform.

Thirdly, the sliding-separation design of the test platform can complete multi-item testing through simple operations, displaying good system integration and high test efficiency. The test platform overcomes the disadvantages of most current RV reducer test benches.

Fourthly, the precision calibration and repeatability test of the test platform verified the stability of the test. The test platform is not only powerful and the measurement results for each parameter are accurate.

Fifthly, the functional test was carried out with the test platform and the measurement results were compared with the data in the enterprise's sample and product manual. The comparison results proved the correctness and effectiveness of the test platform. The experimental results can provide useful data for use in RV reducers.

The study provides a scientific basis for the design improvement, performance prediction and transmission performance improvement of precision reducers.

Acknowledgements

The research was supported by the National Natural Science Foundation of China (Grant No. 51905010) and The National Key Research and Development Program of China (Grant No. 2018YFB2001400).

Metrol. Meas. Syst., Vol. 29 (2022), No. 1, pp. 207–229
DOI: 10.24425/mms.2022.138542

References

[1] Zhang, R., Zhang, C., & Zheng, W. (2018). The status and development of industrial robots. *IOP Conference Series: Materials Science and Engineering*, *423*, 012051. https://doi.org/10.1088/1757-899X/423/1/012051

[2] Gu, J., Huang, D., Tan, J., Liu, J., Wang, S., Li, M., & Xiao, L. (2019). Manufacturing quality assurance for a rotate vector reducer with vibration technology. *Journal of Mechanical Science and Technology*, *33*(5), 1995–2001. https://doi.org/10.1007/s12206-019-0401-3

[3] Blagojevic, M. (2014). Analysis of clearances and deformations at cycloid disc. *Machine Design*, *6*(3), 79–84.

[4] Kudrijavcev, V. N. (1966). Planetary gear train (in Russian). *Mechanical Engineering*, Leningrad.

[5] Bednarczyk, S. (2021). Analysis of the cycloidal reducer output mechanism while taking into account machining deviations. *Proceedings of the Institution of Mechanical Engineers. Part C: Journal of Mechanical Engineering Science*, *235*(23), 7299–7313. https://doi.org/10.1177/09544062211016889

[6] Boguski, B., Kahraman, A., & Nishino, T. (2012). A New Method to Measure Planet Load Sharing and Sun Gear Radial Orbit of Planetary Gear Sets. *Journal of Mechanical Design*, *134*(7). https://doi.org/10.1115/1.4006827

[7] Yang, Z., Mu, Y. & Xiong, Z. (1992). Experimental Research on a New Cycloidal Pin Gear Planetary Transmission Device. *Journal of Dalian Railway University*, 01, 96–98. (in Chinese)

[8] Li, Y. & Wang, J. (2007). Transmission Performance Test of a New Type of Low-Tooth Difference Filter Drive Mechanism. *Machinery Manufacturing*, 11, 66-69. (in Chinese)

[9] Zheng, Y., Xi, Y., Yuan, L., Bu, W., & Li, M. (2017). The design of test bed for RV reducer's dynamic characteristics comprehensive testing. *Chinese Journal of Construction Machinery*, 15(6), 536–541. https://doi.org/10.15999/j.cnki.311926.2017.06.012 (in Chinese)

[10] Gorla, C., Davoli, P., Rosa, F., Longoni, C., Chiozzi, F. & Samarani, A. (2008). Theoretical and Experimental Analysis of a Cycloidal Speed Reducer. *Journal of Mechanical Design*, *130*(11). https://doi.org/10.1115/1.2978342

[11] Jorgensen, F. T., Andersen, T. O., & Rasmussen, P. O. (2008). The Cycloid Permanent Magnetic Gear. *IEEE Transactions on Industry Applications*, *44*(6), 1659–1665. https://doi.org/10.1109/TIA.2008.2006295

[12] Nam, W. & Oh, S. (2011). A design of speed reducer with trapezoidal tooth profile for robot manipulator. *Journal of Mechanical Science and Technology*, *25*(1), 171–176. https://doi.org/10.1007/s12206-010-1112-y

[13] Fan, S., Zhang, L., Wang, L. & Shi, M. (2012) Multifunctional Measurement System for High Precision Planetary Servo Gearhead. *Chinese Journal of Mechanical Engineering*, *25*(2), 398–404. https://doi.org/10.3901/CJME.2012.02.398

[14] Li, C., Cai, S. & Yang, B. (2014). Experimental Study on Backlash and Stiffness of 2K-V Cycloidal Pinwheel Reducer. *Mechanical Design*, *31*(01), 33–36. (in Chinese)

[15] Zhang, Y., Sun, P., Ding, M., Ning, X., Li, Y. & Li, X. (2015). Design and implementation of a test platform for the preloaded assembly of harmonic reducer. *IEEE International Conference on Electronic Measurement & Instruments* (Vol. 1, pp. 522–526). https://doi.org/10.1109/ICEMI.2015.7494264

[16] Qi, H., Wang, X. & Zhang, L. (2016). Development of Comprehensive Parameter Measuring Machine for Precise RV reducer. *Journal of Mechanical Transmission*, *40*(06), 162–165. https://doi.org/10.16578/j.issn.1004.2539.2016.06.036 (in Chinese)

[17] Cao, Y., Liu, G., Yu, H., Mao, H., He, K., & Du, R. (2018). A Novel Comprehensive Testing Platform of RV Reducer. *IEEE International Conference on Information and Automation (ICIA)*, 269–274. https://doi.org/10.13841/j.cnki.jxsj.2014.01.023 (in Chinese)

[18] Catelani, M., Zanobini, A., Z. & Ciani, L. (2010). Uncertainty Interval Evaluation Using the Chi-square and Fisher Distributions in the Measurement Process. *Metrology and Measurement Systems*, *XVII*(2), 195–204. https://doi.org/10.2478/v10178-010-0017-5

[19] Płowucha, W. (2020). Point-plane Distance as Model for Uncertainty Evaluation of Coordinate Measurement. *Metrology and Measurement Systems*, *27*(4), 625–639. https://doi.org/10.24425/mms.2020.134843

[20] Baek, J., Kwak, Y. & Kim, S. (2003). Backlash Estimation of a Seeker Gimbal with Two-stage Gear Reducers. *International Journal of Advanced Manufacturing Technology*, *21*(8), 604–611. https://doi.org/10.1007/s00170-002-1378-z

[21] Yang, Y., Chen, C., & Wang, S. (2018). Response Sensitivity to Design Parameters of RV Reducer. *Chinese Journal of Mechanical Engineering*, *31*(1), 49. https://doi.org/10.1186/s10033-018-0249-y

[22] Hsieh, C. & Jian, W. (2016). The effect on dynamics of using various transmission designs for two-stage cycloidal speed reducers. *Proceedings of the Institution of Mechanical Engineers Part C – Journal of Mechanical Engineering Science*, *230*(4), 665–681. https://doi.org/10.1177/0954406215618984

[23] Marton, L. (2007). On analysis of limit cycles in positioning systems near striebeck velocities. *Mechatronics*, *18*(1), 46–52. https://doi.org/10.1016/j.mechatronics.2007.08.001

[24] Xu, H., Shi Z., Yu B. & Wang H. (2019). Dynamic measurement of the lost motion of precision reducers in robots and the determination of optimal measurement speed. *Journal of Advanced Mechanical Design Systems and Manufacturing*, *13*(3), JAMDSM0044. https://doi.org/10.1299/jamdsm.2019jamdsm0044

[25] Zhang, Y. (2020). *Development of comprehensive performance testing machine for precision reducer*. Master's Thesis, Beijing University of Technology. https://doi.org/10.26935/d.cnki.gbjgu.2020.000387 (in Chinese)

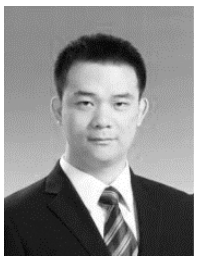

Huijun Yue is a Ph.D., master supervisor at the Beijing University of Technology, Faculty of Materials and Manufacturing – College of Mechanical Engineering and Applied Electronics Technology. His main research interests include gear transmission vibration and noise, precision measurement technology.

Zhaoyao Shi is a Ph.D., professor and doctoral supervisor at the Beijing University of Technology, Faculty of Materials and Manufacturing – College of Mechanical Engineering and Applied Electronics Technology. His main research interests include precision machinery and gear engineering technology.

Xiangkai Wu is a master student at the Beijing University of Technology, Faculty of Materials and Manufacturing – College of Mechanical Engineering and Applied Electronics Technology. His main research interest is gear transmission vibration and noise.

Yue Zhang was a master student at the Beijing University of Technology, Faculty of Materials and Manufacturing-College of Mechanical Engineering and Applied Electronics Technology. His main research interest is precision machinery. He is now working for CRRC SIFANG CO., Ltd.

Metrol. Meas. Syst., Vol. 29 (2022), No. 1, pp. 207–229
DOI: 10.24425/mms.2022.138542

Yong Ye is a professor level senior engineer and master supervisor at the Beijing University of Technology, Faculty of Materials and Manufacturing-College of Mechanical Engineering and Applied Electronics Technology. His main research interest is precision measurement technology.

Lintao Zhang is a senior engineer and master supervisor at the Beijing University of Technology, Faculty of Materials and Manufacturing – College of Mechanical Engineering and Applied Electronics Technology. His main research interest is precision machinery.

Ying Fu is a senior engineer and master supervisor at the Beijing University of Technology, Faculty of Materials and Manufacturing – College of Mechanical Engineering and Applied Electronics Technology. Her main research interest is development of control software.